

Preservation of biological function despite oxidative modification of the apolipoprotein A-I mimetic peptide 4F

C. Roger White,^{1,2,*†} Geeta Datta,^{2,*†} Amanda K. W. Buck,* Manjula Chaddha,*
Gautam Reddy,* Landon Wilson,** Mayakonda N. Palgunachari,* Mohammad Abbasi,*
and G. M. Anantharamaiah*[§]

Departments of Medicine,* Physiology and Biophysics,[†] Biochemistry and Molecular Genetics,[§] and the Targeted Metabolomics and Proteomics Laboratory,** University of Alabama at Birmingham, Birmingham, AL

Abstract Myeloperoxidase (MPO)-derived hypochlorous acid induces changes in HDL function via redox modifications at the level of apolipoprotein A-I (apoA-I). As 4F and apoA-I share structural and functional properties, we tested the hypothesis that 4F acts as a reactive substrate for hypochlorous acid (HOCl). 4F reduced the HOCl-mediated oxidation of the fluorescent substrate APF in a concentration-dependent manner ($ED_{50} \sim 56 \pm 3 \mu\text{M}$). This reaction induced changes in the physical properties of 4F. Addition of HOCl to 4F at molar ratios ranging from 1:1 to 3:1 reduced 4F band intensity on SDS-PAGE gels and was accompanied by the formation of a higher molecular weight species. Chromatographic studies showed a reduction in 4F peak area with increasing HOCl and the formation of new products. Mass spectral analyses of collected fractions revealed oxidation of the sole tryptophan (Trp) residue in 4F. 4F was equally susceptible to oxidation in the lipid-free and lipid-bound states. To determine whether Trp oxidation influenced its apoA-I mimetic properties, we monitored effects of HOCl on 4F-mediated lipid binding and ABCA1-dependent cholesterol efflux. Neither property was altered by HOCl. These results suggest that 4F serves as a reactive substrate for HOCl, an antioxidant response that does not influence the lipid binding and cholesterol effluxing capacities of the peptide.—White, C. R., G. Datta, A. K. W. Buck, M. Chaddha, G. Reddy, L. Wilson, M. N. Palgunachari, M. Abbasi, and G. M. Anantharamaiah. **Preservation of biological function despite oxidative modification of the apolipoprotein A-I mimetic peptide 4F.** *J. Lipid Res.* 2012. 53: 1576–1587.

Supplementary key words hypochlorous acid • tryptophan • oxidation • cholesterol efflux

Myeloperoxidase (MPO), an abundant heme protein released by activated leukocytes, catalyzes the oxidation of chloride ions by hydrogen peroxide (H_2O_2) to yield hypochlorous acid (HOCl). MPO has been identified as a biomarker for pathological conditions including sepsis, ischemic injury and atherosclerosis (1–4). Increased circulating levels of MPO are associated with increased coronary risk, and MPO colocalizes with macrophages in human atherosclerotic lesions (1, 2). HOCl is a potent oxidant whose cellular targets of action include thiols, amines, nucleotides, unsaturated fatty acids and lipoproteins (5). With respect to lipoprotein metabolism, HOCl impairs both LDL and HDL function. HOCl oxidizes apolipoprotein (apo) B100 and lipid components of LDL particles, resulting in increased scavenger receptor uptake of LDL by macrophages and the development of fatty lesions (6, 7). The HOCl-dependent oxidation of HDL converts it to a form that is proatherogenic (8–11). Dysfunctional HDL particles demonstrate a reduced capacity to mediate ATP-binding cassette transporter A1 (ABCA1)-dependent cholesterol efflux and are resistant to metabolism by hepatic enzyme systems (12–17). MPO and HOCl also inhibit the activity of the HDL-associated enzyme lecithin cholesterol acyl transferase (LCAT), thus attenuating the formation of mature α -HDL particles (18). The MPO-catalyzed oxidation of HDL also attenuates anti-apoptotic and anti-inflammatory effects of the lipoprotein (11). These changes are associated with reduced binding of HDL to scavenger receptor class B1 (SR-B1).

Data suggest that the formation of dysfunctional HDL by MPO and HOCl is due principally to changes in the protein components of the particle (whereas higher concentrations may induce changes in the lipid composition

This work was supported by National Institutes of Health Grants GM-082952 (G.D./C.R.W.), HL-34345 (G.M.A.), T32 HL-007457 (A.K.W.B.), S10 RR-027822-01, and S10 RR-13795. Its contents are solely the responsibility of the authors and do not necessarily represent the official views of the National Institutes of Health. This work was also supported by the University of Alabama at Birmingham Health Services Foundation General Endowment Fund. G.M.A. is a principal for Bruin Pharma.

Manuscript received 12 March 2012 and in revised form 8 May 2012.

Published, JLR Papers in Press, May 15, 2012

DOI 10.1194/jlr.M026278

Abbreviations: Cl-Tyr, chlorotyrosine; DiOia, dioxindolylalanine; HOCl, hypochlorous acid; MPO, myeloperoxidase; N-Tyr, nitrotyrosine; Oia, oxindolylalanine; Phe, phenylalanine; SR-B1, scavenger receptor class B1; TFA, trifluoroacetic acid; Trp, tryptophan; Tyr, tyrosine.

¹To whom correspondence should be addressed.

e-mail: crwhite@uab.edu

²C. R. White and G. Datta contributed equally to this work.

Copyright © 2012 by the American Society for Biochemistry and Molecular Biology, Inc.

of the particle) (9). In this regard, immunohistochemical studies demonstrate the colocalization of apoA-I and HOCl-modified epitopes in atherosclerotic lesions (8, 12, 19). Oxidation of apoA-I results in the formation of high molecular weight aggregates (9). Further, exogenously generated reactive carbonyls may covalently modify apoA-I by cross-linking lysine residues, resulting in loss of ABCA1-mediated cholesterol efflux (15). The sequence of apoA-I possesses numerous targets for MPO and HOCl action, as determined by mass spectrometry (16–19). Analysis of apoA-I isolated from human atheroma shows the presence of oxidized tryptophan (Trp), lysine, methionine, and tyrosine (Tyr) residues (20). HOCl induces similar modifications to amino acids under *in vitro* conditions but with variable reactivities (8, 9, 18). In this respect, kinetic studies have shown that HOCl reacts with Trp and Tyr yielding second order rate constants of 1.1×10^4 and $44 \text{ k}_2/\text{M}^{-1}\text{s}^{-1}$, respectively (21). Under the same reaction conditions, the rate of reaction of HOCl with phenylalanine (Phe) was negligible (21). In light of observations that HDL isolated from patients with coronary artery disease contains elevated levels of nitrotyrosine (N-Tyr) and chlorotyrosine (Cl-Tyr), several studies have focused on the role of MPO and HOCl in the modification of Tyr residues in apoA-I (16, 19). Although N-Tyr and Cl-Tyr are both markers of redox injury, data suggest that tyrosine chlorination, but not nitration, is a critical determinant of impaired ABCA1-dependent cholesterol efflux (16, 22). It was proposed that chlorination of up to two of the seven Tyr residues in apoA-I plays a critical role in the inhibition of ABCA1-mediated cholesterol efflux (16, 23). Tyr chlorination under these conditions was dependent on the reaction of HOCl with the KXXY amino acid motif (24). Three such regions are present in apoA-I (24). Other studies suggest that although Cl-Tyr formation in apoA-I may represent a marker for dysfunctional HDL, Tyr chlorination per se is not a mechanism underlying the inhibition of ABCA1-mediated cholesterol efflux (25). Rather, these studies indicated that the fundamental mechanism underlying the loss of HDL function was the oxidation of Trp residues in the protein (25).

The development of apo mimetic peptides represents a potentially new therapeutic approach for the treatment of lipid disorders. The synthetic peptide 4F, whose structure is based on the helical repeating domains of apoA-I, possesses anti-inflammatory and antioxidant properties and dramatically reduces lesion formation in dyslipidemic mouse models (26). 4F is an effective mediator of ABCA1-mediated cholesterol efflux (27,28). A recent study demonstrates that an additional property of the peptide is its ability to avidly bind and neutralize oxidized lipids (29). The class A amphipathic helical structure of 4F is similar to the amphipathic helical domains of apoA-I in that it contains a similar composition of redox sensitive amino acid residues including the KXXY motif. A goal of the current study, therefore, was to test whether 4F possesses novel antioxidant properties and how HOCl-dependent oxidation impacts the lipid-binding and ABCA1-mediated cholesterol effluxing properties of this peptide.

Materials

1-Palmitoyl-2-oleoyl-*sn*-glycero-3-phosphocholine (POPC) was obtained from Avanti Polar Lipids. (Alabaster, AL). Sodium hypochlorite was from Sigma. Superose 6 columns were from Amersham Biosciences (NJ). 2-[6-(4-aminophenoxy)-3-oxo-3H-xanthen-9-yl]benzoic acid (APF) was obtained from Cayman Chemicals. ^3H -cholesterol was from American Radiochemicals (St. Louis, MO). Hypochlorous acid concentration was determined by monitoring the absorbance of hypochlorite at 292 nm ($\epsilon = 350 \text{ M}^{-1}\text{cm}^{-1}$) in 0.1N NaOH using a Beckman diode array spectrophotometer Model DU 7000.

Peptide synthesis

The apoA-I mimetic peptide 4F, whose amino acid sequence is Ac-DWFKAFYDKVAEKFKKEAF-NH₂, was synthesized by the solid phase peptide synthesis method as previously described (30). ^{14}C -4F was synthesized as described previously (31). The modified peptide 4F [W→F] (Ac-DEFKAFYDKVAEKFKKEAF-NH₂) was synthesized by substituting phenylalanine (Phe/F) for tryptophan (Trp/W) and was used as a control peptide. Peptide purity was ascertained by mass spectral analysis and analytical HPLC. Peptide concentration for 4F and the 4F [W→F] analog was determined using $\epsilon_{280} = 7,300 \text{ M}^{-1}\text{cm}^{-1}$ and $\epsilon_{264} = 1,280 \text{ M}^{-1}\text{cm}^{-1}$, respectively. Both peptides were endotoxin free as determined by the Limulus assay using the QCL-1000 kit (Lonza).

Peptide effects on HOCl-dependent oxidation of APF

In initial studies, effects of 4F and 4F [W→F] on HOCl-dependent oxidation were assessed. Briefly, 4F or 4F [W→F] (10–300 μM) was added to a physiological salt solution containing APF (1.6 $\times 10^{-2}$ mM). HOCl (100 μM) was then added to initiate the oxidation of nonfluorescent APF to yield fluorescein. Fluorescein fluorescence was then monitored on a Bio-Tek Synergy HT microplate reader using $\lambda_{\text{ex}} = 480 \text{ nm}$ and $\lambda_{\text{em}} = 515$.

Electrophoresis studies

To determine whether HOCl induces changes in the physical characteristics of 4F and 4F [W→F], native and oxidized peptides were analyzed by denaturing gel electrophoresis. HOCl was added to 4F or 4F [W→F] at HOCl:peptide molar ratios ranging from 1:1 to 3:1. Residual HOCl activity was quenched by addition of taurine (100 μM) after 15 min. Native and HOCl-modified peptides (14 μg) were then loaded onto 4–20% SDS-Tris glycine gels and stained with Coomassie blue. Gels were destained using MeOH:acetic acid:H₂O. See Blue Plus 2 low molecular weight markers (Invitrogen) were loaded onto gels for identification of bands. Gels were scanned, and band intensity analysis was performed using LabWorks software (Lablogics V4.6). In some experiments, ^{14}C -labeled 4F was oxidized by HOCl prior to electrophoretic separation. Bands were cut from SDS gels, and the distribution of radioactive counts was determined by scintillation counting. Data are expressed as a percentage of radioactive counts in the 4F band in the absence of HOCl treatment.

Chromatography

To further characterize HOCl-induced modifications to 4F and 4F [W→F], native and oxidized peptide samples were analyzed by analytical, reverse phase high pressure column chromatography using a Beckman-Coulter HPLC system. HOCl was added to 4F or 4F [W→F] at molar ratios ranging from 1:1 to 3:1. Samples (25 μg) were injected onto a C18 column (Vydak, 4.6 \times 250 mm, particle size 5 μm) and eluted with acetonitrile in H₂O [0.1% trifluoroacetic acid (TFA)] using a 35–55% gradient

(40 min). Peptide bond absorbance was monitored at 220 nm. In subsequent studies, 600 µg peptide was injected onto the column to obtain sufficient material for analysis by mass spectrometry. Peak fractions (1.0 ml) were pooled from 3 individual HPLC runs and lyophilized. To determine the relative susceptibility of 4F and apoA-I to oxidation, the HOCl-induced loss of Trp and Tyr absorbance was monitored at 280 nm. HOCl was added to samples of 4F or apoA-I (1 mg/ml each) at a 3:1 molar ratio for time periods ranging from 30 s to 15 min. In some experiments, 4F and apoA-I were mixed with 1,2-Dimyristoyl-sn-glycero-3-phosphorylcholine (DMPC:1:1 mol/mol) to form lipid complexes prior to HOCl addition. At the end of each time point, taurine was added to quench unreacted HOCl. The relative decay of HOCl-treated 4F or apoA-I was then assessed by HPLC at A_{280} .

Mass spectrometry

Native and oxidized 4F and 4F [W→F] samples were initially analyzed by MALDI-TOF mass spectrometry using the Applied Biosystems Voyager DE-Pro in the reflector positive ion mode (Foster City, CA) at 20 Hz. Material obtained from novel peaks identified by HPLC were resuspended in a 1:10 dilution of α -cyano-4-hydroxycinnamic acid in 0.1% TFA and plated for analyses.

The mass range selected was from 1,000–4,000 m/z with 500 spectra/sample collected. Post analysis data processing was performed using Voyager Data Explorer software (version 3.40).

Sequence analysis of oxidized peptides was performed using NanoLC-tandem mass spectrometry. An aliquot (2 µl) of each digest was loaded onto a 2 cm \times 75 µm i.d. PepMap100 C₁₈ reverse-phase trap cartridge (Dionex, Sunnyvale, CA) at 2 µl/min using an Eksigent autosampler. After washing the cartridge for 4 min with 0.1% formic acid in ddH₂O, the bound peptides were flushed onto a 15 cm \times 75 µm i.d. PepMap100 C₁₈ reverse-phase analytical column (Dionex) with a 40 min linear (5–50%) acetonitrile-H₂O gradient in the presence of 0.1% formic acid at 300 nl/min using an Eksigent Nano1D+ LC. (Dublin, CA). The column was washed with 90% acetonitrile-0.1% formic acid for 15 min and then reequilibrated with 5% acetonitrile-0.1% formic acid for 30 min. The Applied Biosystems 5600 Triple-TOF mass spectrometer (AB-Sciex, Toronto, Canada) was used to analyze the peptide digest. Eluted peptides were subjected to a time-of-flight survey scan from 400–1,250 m/z to determine the top twenty most intense ions for MS/MS analysis. Product ion time-of-flight scans at 50 msec were carried out to obtain the tandem mass spectra of the selected parent ions over the range from m/z 400–2,000. Spectra are centroided and deisotoped by Analyst software, version TF (Applied Biosystems). A β -galactosidase trypsin digest was used to establish and confirm the mass accuracy of the mass spectrometer.

Fluorescence properties of 4F

The Trp fluorescence emission spectrum for native and HOCl-modified 4F (1:1-3:1) were monitored using λ_{ex} = 295 nm and λ_{em} = 349 nm.

Phospholipid clarification

Effects of native and oxidized 4F and 4F [W→F] on the turbidity of POPC (100 µM) multilamellar vesicles (MLV) was measured in PBS by light scattering. For oxidation studies, HOCl was added to 4F or 4F [W→F] at molar ratios ranging from 1:1 to 3:1. The peptide solutions were then added to MLVs of POPC (1:1 mol/mol ratio), and phospholipid turbidity clarification was measured every 30 s for 30 min using an SLM-AMINCO 8100 Spectrofluorometer (SLM Instruments). Representative light scattering profiles for each peptide are presented.

Circular dichroism spectroscopy

CD spectra were recorded using JASCO J-815 spectropolarimeter equipped with a Peltier-type temperature control system (JASCO model PTC-423s/15). CD spectra were recorded every nanometer from 260 nm to 195nm using a cell with a 0.1 cm path length. Spectra were recorded at 25°C and represent the average of two scans. Peptide concentrations were 50 µM in PBS (pH 7.4). Mean residue ellipticity ($[\theta]_{MRE}$) (degcm²/dmol) at θ_{222} was calculated using the following equation:

$$[\theta]_{MRE} = (MRW \times \theta) / (10 \text{ cl})$$

where MRW is the mean residue weight (peptide molecular weight divided by the number of amino acids); θ is the observed helicity in degrees; c is concentration of peptide in g/ml; and l is the path length in centimeters. Percentage helicity was calculated using the following equation, as previously described (30):

$$\text{Percent } \alpha \text{ Helix} = ([MRE \theta_{222} + 3,000] / [36,000 + 3,000]) \times 100$$

ABCA1-mediated cholesterol efflux

4F- and 4F [W→F]-mediated cholesterol efflux were measured following the procedure of Kritharides et al. (32). Briefly, THP-1 monocytes were seeded at 10⁶ cells/well in 6-well plates. Acetylated LDL, radiolabeled with ³H-cholesterol, was added to cells for 24 h at 37°C. 8-bromo cAMP (300 µM) was then added to cells for an additional 24 h to induce ABCA1 expression. Cells were then incubated with 100 µg/ml 4F or 100 µg/ml 4F [W→F] for 24 h at 37°C in lipoprotein-depleted medium containing 2 mg/ml BSA. In some experiments, HOCl was incrementally added to 4F or 4F [W→F] resulting in HOCl:peptide molar ratios ranging from 1:1 to 3:1. These HOCl-modified samples were then added to THP-1 cells for 24 h. At the end of this time period, media and cell lysates were collected for ³H-cholesterol scintillation counting to determine amount of cholesterol effluxed from cells. Efflux data was normalized and expressed as a percentage of total counts effluxed by 4F or 4F [W→F]. To test whether potentially saturating amounts of native and oxidized peptides (100 µg/ml) were masking a more subtle effect of oxidation on efflux, we performed concentration response experiments. HOCl was added to 4F or 4F [W→F] (10, 25, 50, and 100 µg/ml) at an HOCl:peptide molar ratio of 3:1. Native and oxidized peptides were then added to radiolabeled THP-1 cells for measurement of cholesterol efflux.

Statistical methods

All results are reported as the mean \pm SEM. Statistical analysis was performed using SigmaStat 3.5 software (Systat Software). Differences between the groups were assessed by one-way ANOVA (ANOVA) with *post hoc* testing (Student-Neuman-Keuls test). A *P* value < 0.05 was considered statistically significant.

RESULTS

MPO-derived HOCl has been shown to oxidatively modify apoA-I. As apoA-I and the apoA-I mimetic peptide 4F share similar structural properties, we tested the hypothesis that 4F serves as a reactive substrate for HOCl. In initial experiments, we assessed effects of varying 4F concentration on the capacity of reagent HOCl to oxidize the

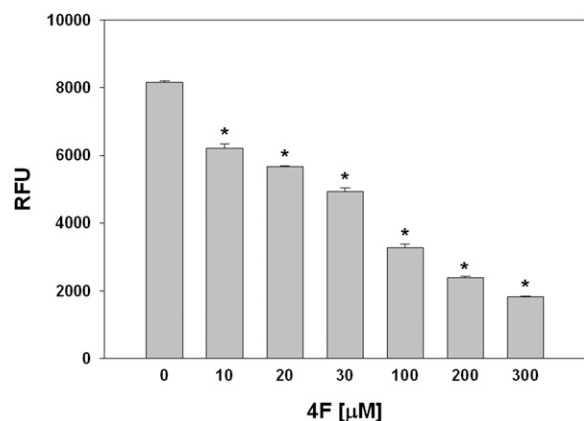


Fig. 1. 4F and 4F [W→F] attenuate the oxidative modification of APF by HOCl. 4F inhibited the HOCl-dependent oxidation of APF to fluorescein in a concentration-dependent manner. Increasing concentrations (10–300 μM) of peptide were added to PBS containing APF. HOCl (100 μM) was then added to initiate the oxidation of nonfluorescent APF to yield fluorescein. Fluorescein fluorescence was monitored using $\lambda_{\text{ex}} = 480 \text{ nm}$ and $\lambda_{\text{em}} = 515$. Data are the mean \pm SEM ($n = 4$ for each peptide treatment). * $P < 0.05$ compared with all other peptide concentrations.

nonfluorescent substrate APF to yield the fluorescent compound fluorescein. 4F reduced fluorescein formation in a concentration-dependent manner (Fig. 1). The ED_{50} for inhibition of HOCl-dependent APF oxidation by 4F was $56 \pm 3 \mu\text{M}$. These results suggested that 4F actively competes with APF for reaction with HOCl. We next examined effects of HOCl-dependent oxidation on the physical properties of 4F. HOCl was added to 4F at molar ratios of 1:1, 2:1, and 3:1. Taurine was added to samples after 15 min to quench unreacted HOCl, followed by separation on denaturing gels. Fig. 2 depicts a representative SDS gel showing

a single band for unmodified 4F (HOCl:4F ratio = 0:1) corresponding to its native mass (2.31 kDa). As the molar ratio of HOCl was increased, the density of the native 4F band was significantly reduced and was accompanied by an increase in the density of a higher molecular weight species (Fig. 2A). Separation of ^{14}C -labeled 4F on denaturing gels showed that the radioactivity associated with the lower molecular weight 4F band decreased with HOCl addition and was transferred to the higher molecular weight species (Fig. 2B). The apparent increase in the molecular mass of oxidized 4F suggested that HOCl treatment induced the cross-linking of the peptide.

We next analyzed HOCl-induced modifications to 4F by analytical HPLC. Chromatographic separation of native 4F yielded a principal peak with a retention time of approximately 27 min (Fig. 3A). Addition of HOCl to 4F at molar ratios of 1:1, 2:1, and 3:1 reduced the integrated peak area for 4F by 36, 60, and 67%, respectively (Fig. 3A, inset). The chromatogram for HOCl-modified 4F (3:1 reaction product) is depicted in Fig. 3B and revealed the formation of additional products. These new peaks eluted from the column prior to native 4F, suggesting a decrease in hydrophobicity. This is supported by the lack of characteristic Trp fluorescence after HOCl treatment, as shown in Fig. 4A. A variety of oxidized 4F products were identified in these fractions by MALDI-TOF mass spectrometry (Table 1). MS analysis of the principal chromatographic peak E (see Fig. 3B) revealed significant oxidative modification to the sole Trp residue in 4F. This was confirmed by studies that showed HOCl reduced the Trp fluorescence of 4F in a concentration-dependent manner (Fig. 4A). At HOCl:4F molar ratios of 1:1, 2:1, and 3:1, the fluorescence (predominantly due to the sole Trp residue) of 4F was reduced by 56, 80, and 91%, respectively, compared with

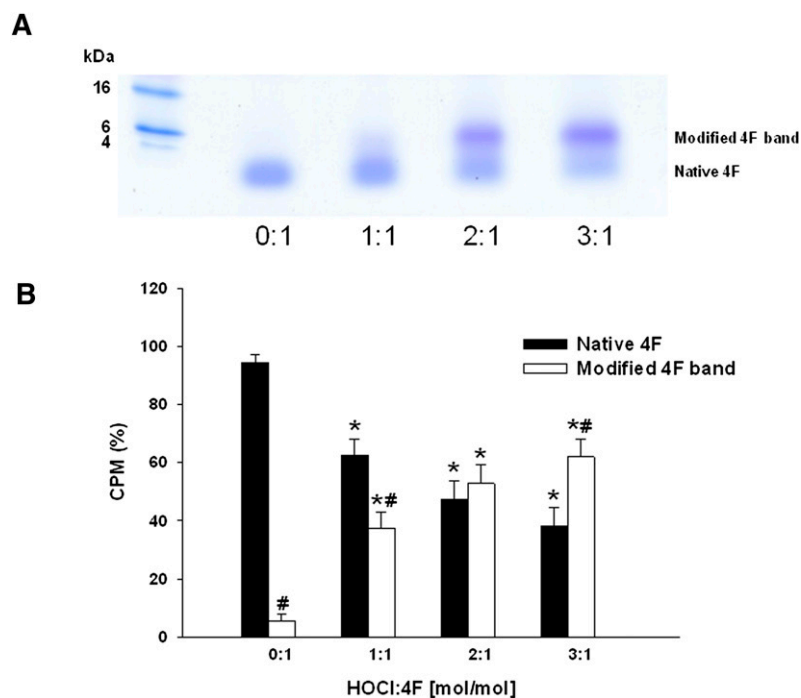


Fig. 2. Effects of HOCl on the electrophoretic properties of 4F. Addition of increasing concentrations of HOCl to 4F resulted in a decrease in native 4F band density when separated on an SDS-PAGE gel. This was accompanied by the appearance of a new band with a higher molecular weight (panel A). Native and HOCl-modified ^{14}C -labeled 4F were separated on denaturing gels. An increase in the ratio of HOCl:4F was associated with increased incorporation of the radiolabel in the higher molecular weight band. Data represent the percentage cpm present in each band and are means \pm SEM for $n = 3$ gels. * $P < 0.05$ in cpm for HOCl-modified bands compared with bands in the absence of HOCl treatment (0:1). # $P < 0.05$ compared with cpm in the low molecular weight, native 4F band (panel B).

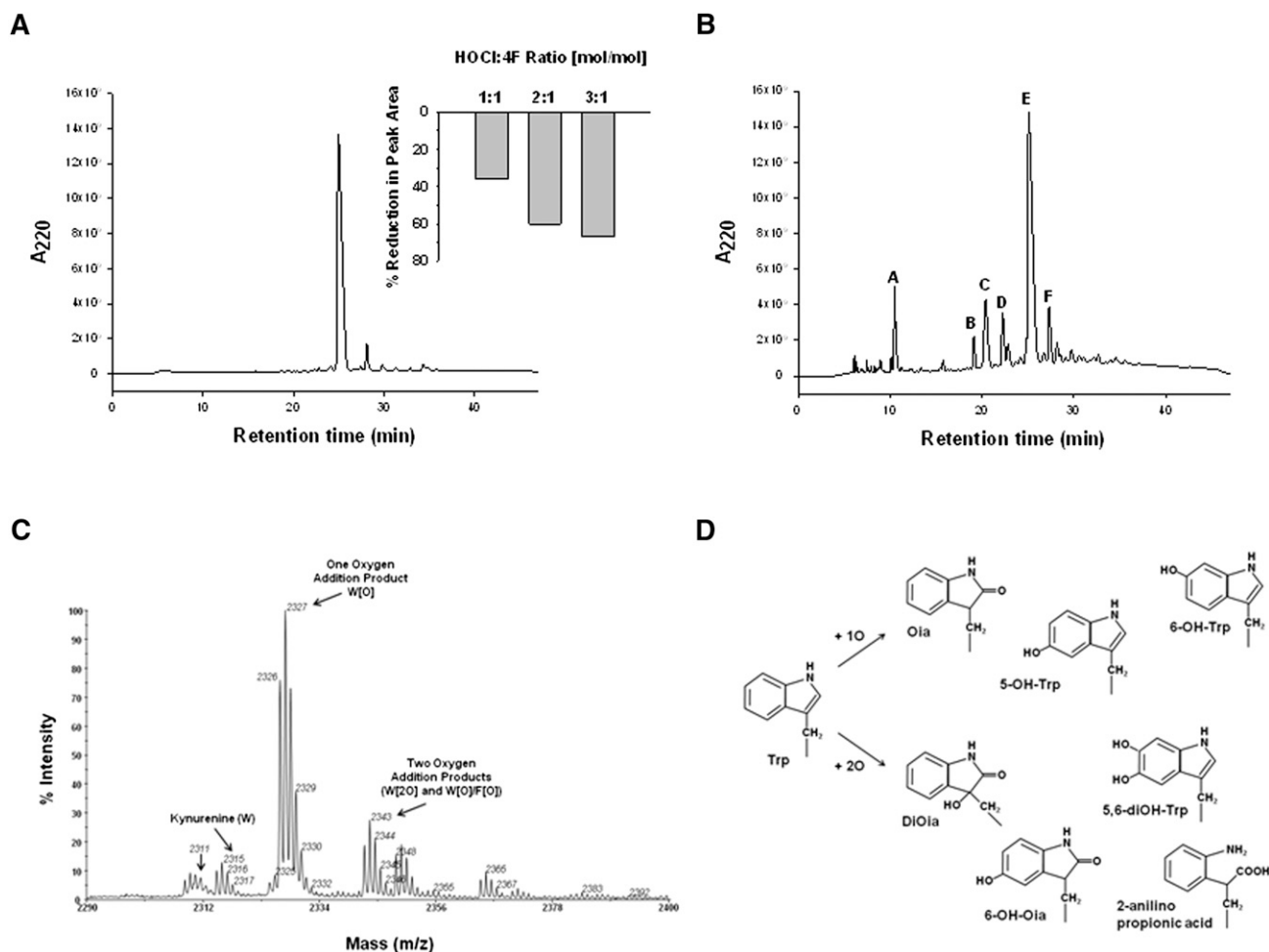


Fig. 3. HOCl alters the physical characteristics of 4F. 4F and its oxidation products were analyzed by chromatography and mass spectrometry. HPLC separation of 4F (25 μ g) yielded a principal peak with a retention time of 27 min. Addition of HOCl to 4F (1:1–3:1 mol/mol) reduced the integrated area of the native 4F peak (panel A). The chromatographic profile for HOCl-modified 4F (3:1 mol/mol) revealed the formation of new 4F products (panel B). Peaks obtained from the separation depicted in panel B were collected and analyzed by MALDI-TOF mass spectrometry. The m/z scan for the predominant peak E (27 min retention time) contained multiple products including one- and two-oxygen addition products. Kynurenine and unmodified 4F were also present in lower abundance (panel C). Analysis of HPLC peaks A–F revealed one- and two-oxygen addition products of Trp with similar m/z ratios but different retention times. These oxidized products likely represent the addition of oxygen to different sites on the indole ring. Proposed structures of these Trp metabolites are depicted in panel D.

peak fluorescence in the absence of HOCl, indicating almost complete modification of Trp under these conditions (Fig. 4A).

The time-dependence for the HOCl-induced decay of 4F (3:1 mol/mol) was monitored by HPLC. Fig. 4B shows that HOCl rapidly reduced Trp absorbance (A_{280}) in 4F within 30 s after addition. The maximal reduction in A_{280} under these conditions was 74% at the 15 min time point. We additionally monitored effects of HOCl on the stability of apoA-I. The initial rate of decay for HOCl-treated apoA-I (3:1 mol/mol) was similar to that of 4F, whereas the maximal reduction in A_{280} (57%) was reduced compared with 4F. The increased susceptibility of lipid-free 4F to oxidation may be due to the fact that, on a molar basis, the peptide contains approximately three times as many Trp residues as apoA-I. In the presence of DMPC, decay profiles for 4F and apoA-I were similar and showed a maximum reduction in A_{280} of 70 and 73%, respectively (Fig. 4B).

These data suggest that on an equimolar basis and in the presence of lipid, 4F and apoA-I are equally susceptible to HOCl-induced oxidation.

MALDI-TOF mass spectrometry was employed to assess oxidative modifications to Trp in greater detail. MS analysis of native 4F revealed a species with the expected m/z ratio of 2,311 in the positive ion mode. Addition of HOCl to 4F (3:1 mol/mol) resulted in the formation of several novel products (Table 1). A one oxygen addition product of Trp (W[O]) with a net gain of 16 mass units (2,327 m/z) was present in greatest abundance in chromatographic peak E (Fig. 3B, C). The formation of W[O] in 4F was confirmed by MS/MS sequence analysis. Although the specific site of oxygen addition to Trp cannot be deduced from MS studies, it is likely that oxygen addition results in the formation of oxindolylalanine (Oia), 5-OH-tryptophan or 6-OH-tryptophan. Structures for these W[O] metabolites are presented in Fig. 3D. Two 2O addition products

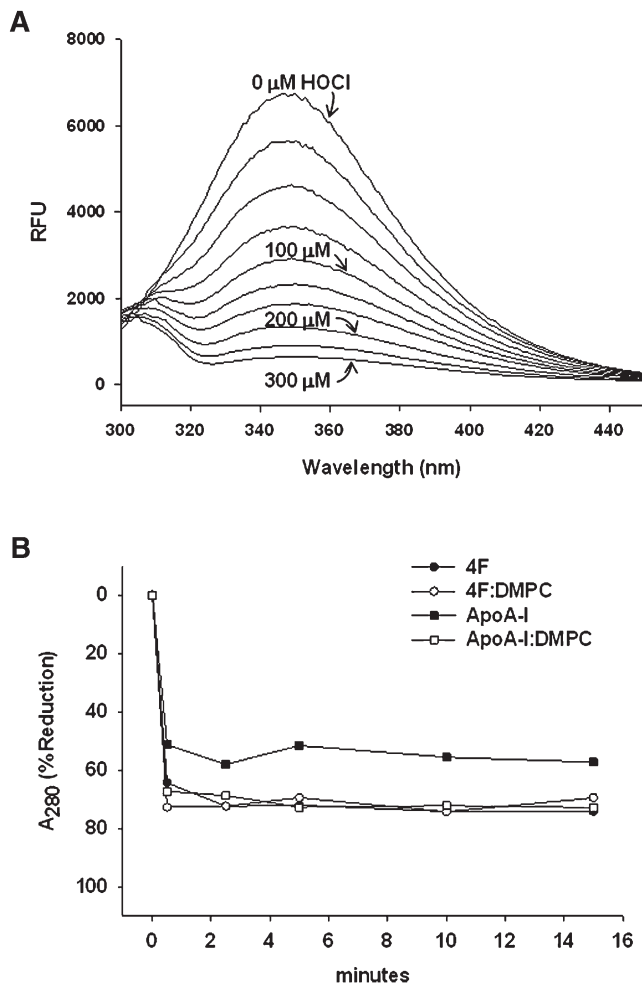


Fig. 4. HOCl alters the spectral properties of 4F. (A) The Trp fluorescence emission spectrum for 4F (100 μ M) was monitored using $\lambda_{\text{ex}} = 295$ nm and $\lambda_{\text{em}} = 349$ nm. Representative spectra show that addition of HOCl to 4F in solution (up to 3:1 mol/mol) progressively reduced peak fluorescence, suggesting modification of Trp ring structure. (B) Lipid-free and lipid-bound (DMPC) 4F or apoA-I (1 mg/ml each) were prepared and then exposed to HOCl at a molar ratio of 3:1 for time periods between 30 sec and 15 min. The oxidation-induced loss of Trp and Tyr absorbance at A_{280} was monitored. The initial rate of decay for both lipid-free 4F (filled circles) and apoA-I (filled squares) was similar and near maximal after 30 sec. The maximal reduction in A_{280} under these conditions was 74% for 4F and 57% for apoA-I. Decay curves for 4F:DMPC (open circles) and apoA-I:DMPC (open squares) displayed similar kinetic profiles as lipid-free 4F.

of 4F (2,343 m/z) were also present to a lesser degree in fraction E. One species bearing the W[2O] modification was identified. This HOCl-derived product represents di-oxindolylalanine (DiOia) or an alternate W[2O] product depicted in Fig. 3D. The other 2O addition product (2,343 m/z) in peak E was characterized by the addition of a single oxygen to Trp and to one of the four Phe residues (W[O]/F[O]). The Trp metabolite kynurenine and unmodified 4F were also noted in peak E in lower abundance. MS analysis of other chromatographic fractions depicted in Fig. 3B revealed the presence of 4F bearing W[O], W[2O], and W[O]/F[O] modifications as well as oxidized and nonoxidized cleavage products of 4F (Table 1). Oxidized 4F

TABLE 1. Reaction products of 4F (Ac-DWFKAFYDKVAEKFKAEF-NH₂) generated by the addition of HOCl

Fraction	4F Reaction Products
A	FKAFYDKVAEKFKAEF-NH₂
B	Ac-DW[Kyn]FKAFYDKVAEKFKAEF-NH₂
C	FKAFYDKVAEKFKAEF-NH ₂ W[O]FKAFYDKVAEKFKAEF-NH ₂ W[2O]FKAFYDKVAEKFKAEF-NH ₂ Ac-DW[O]F[O]KAFYDKVAEKFKAEF-NH₂ Ac-DW[O]FKAFYDKVAEKFKAEF-NH ₂
D	Ac-DW[O]FKAFYDKVAEKFKAEF-NH₂
E	Ac-DW[2O]FKAFYDKVAEKFKAEF-NH ₂ Ac-DW[Kyn]FKAFYDKVAEKFKAEF-NH ₂ Ac-DW[O]FKAFYDKVAEKFKAEF-NH₂ Ac-DW[2O]FKAFYDKVAEKFKAEF-NH ₂ Ac-DW[O]F[O]KAFYDKVAEKFKAEF-NH ₂
F	DWFKAFYDKVAEKFKAEF-NH ₂ W[O]FKAFYD(-H₂O)KVAEKFKAEF-NH₂ W[2O]FKAFYDKVAEKFKAEF-NH ₂ Ac-DW[O]FKAFYDKVAEKFKAEF-NH ₂

Chromatographic peaks depicted in Fig. 3B were collected, lyophilized, and reconstituted for MALDI-TOF MS analysis. The predominant species present in each fraction is bolded. The conversion of W to kynurenine is denoted by W[Kyn].

metabolites with similar m/z ratios were identified in different collected fractions. For example, three W[O] metabolites of 4F were observed in different peaks (C, D, E, and F in Fig. 3B). This likely reflects the addition of oxygen to three different sites on W, thus imparting differing degrees of hydrophobicity and elution from the column. Finally, peak F contained a product with a molecular mass of 4,616 kDa. This appears to correspond to a 4F dimer, with an epsilon-NH₂ in one strand interacting with the carbonyl group in the other strand to form a Schiff base adduct on both ends of a head-to-tail dimer. This is consistent with the formation of the higher molecular weight product seen with HOCl treatment on SDS gels (Fig. 2A).

Because these data suggested that Trp is a critical site for HOCl-dependent oxidation, additional studies were performed using the modified peptide 4F [W→F]. This peptide is identical to 4F with the exception that the Trp residue is replaced by Phe. 4F [W→F] displayed a similar concentration dependence ($ED_{50} = 51 \pm 9 \mu\text{M}$) as 4F for inhibiting the HOCl-dependent oxidation of APF (Fig. 5A). In contrast to HOCl-modified 4F, oxidation of 4F [W→F] did not alter its mobility on SDS gels, suggesting the relative preservation of size (Fig. 5B). HPLC separation of native 4F [W→F] revealed a single peak with a retention time of approximately 21 min (Fig. 5C). In contrast to the elution profile noted with oxidized 4F, oxidized 4F [W→F] products were observed with a prolonged retention time, suggesting increased hydrophobicity (Fig. 5D). Analysis of the principal peak A revealed unmodified 4F [W→F] peptide (Fig. 5D, Table 2). Overall, 4F [W→F] was more resistant to HOCl-dependent modification. Table 2 shows that unmodified 4F [W→F] was present in all the peaks except B. To collect adequate material for this analysis, a relatively large amount of peptide (600 μg) was injected onto the HPLC column. It is possible that the appearance of the unmodified parent molecule in multiple peaks may be due to column overloading. HOCl-modified 4F [W→F] products were identified in peaks B and F and were

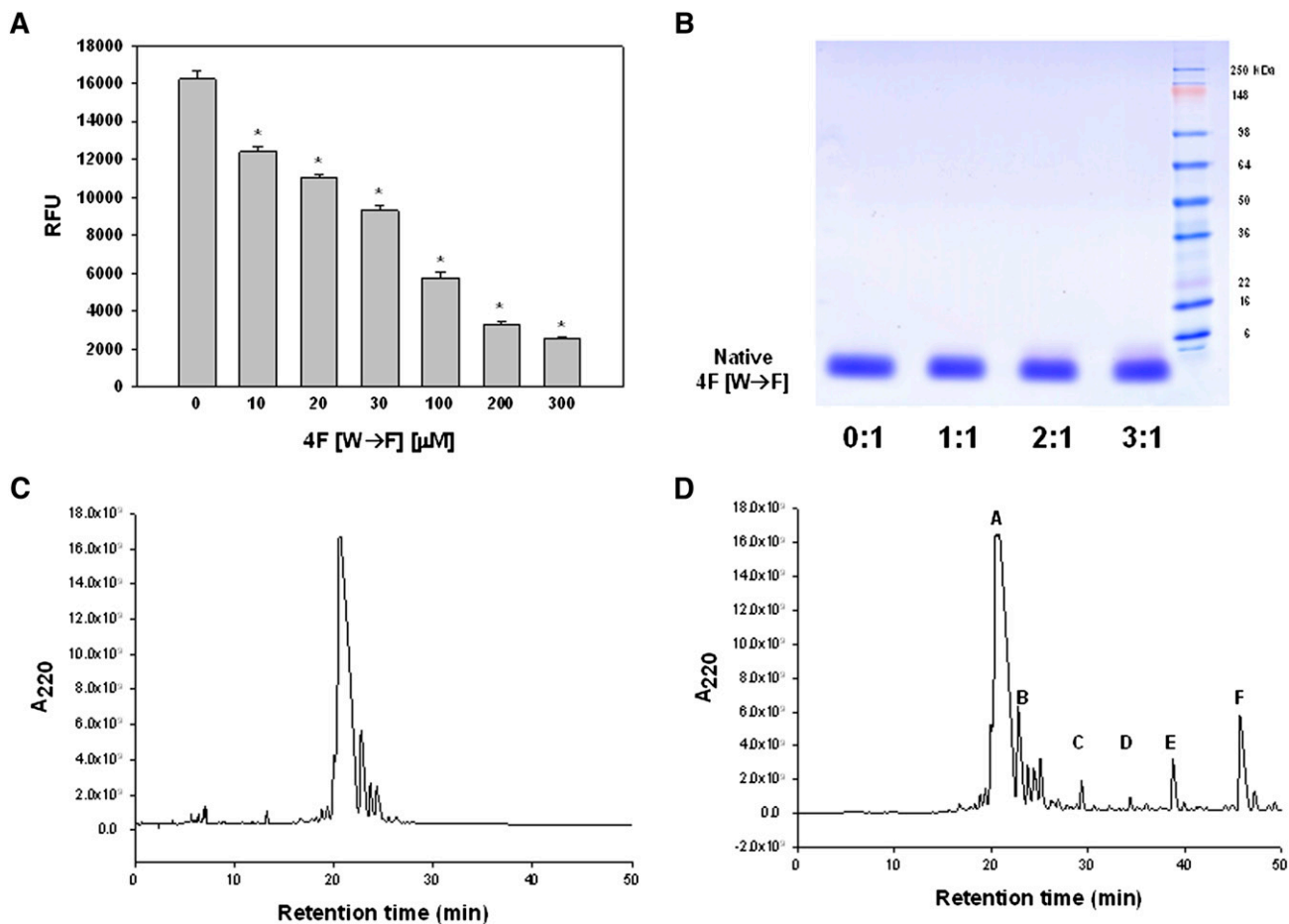


Fig. 5. Effects of HOCl on the physical properties of the 4F [W→F] peptide. 4F [W→F] inhibited the HOCl-dependent oxidation of APF to fluorescein in a concentration-dependent manner (panel A). Native and HOCl-treated 4F [W→F] were separated on denaturing SDS gels. A representative gel shows that, in contrast to 4F, HOCl treatment did not alter the position of 4F [W→F] (panel B). HPLC separation of 4F [W→F] yielded a principal peak with a retention time of 21 min (panel C). HOCl induced the formation of new 4F [W→F] products that eluted from the column at later time points. MALDI-TOF mass spectrometry revealed the presence of unmodified 4F [W→F] in all peaks. Peaks B and F contained 4F [W→F] metabolites bearing chlorinated tyrosine (Y[Cl]) residues (panel D).

characterized by the chlorination of a tyrosine residue with only minor evidence for oxidation (Table 2).

In a final series of experiments, we assessed effects of native and oxidized 4F and 4F [W→F] on phospholipid clarification and cholesterol efflux. **Fig. 6A** shows that the ability of 4F to clarify a POPC solution was unaffected by HOCl treatment. Consistent with this, there was no effect

TABLE 2. Reaction products of 4F [W→F] 4 (Ac-DFFKAFYDKVAEKFKKEAF-NH₂) generated by the addition of HOCl

Fraction	4F [W→F] Reaction Products
A	Ac-DFFKAFYDKVAEKFKKEAF-NH₂
B	FFKAFYDKVAEKFKKEAF-NH₂ Ac-DFFKAFY[Cl]DKVAEKFKKEAF-NH₂
C	Ac-DFFKAFYDKVAEKFKKEAF-NH₂ Ac-DFFKAFYDKVAEKFKKEAF[2O]NH ₂
D	Ac-DFFKAFYDKVAEKFKKEAF-NH₂
E	Ac-DFFKAFYDKVAEKFKKEAF-NH₂ Ac-DFFKAFYDKVAEKFKKEAF[2O]NH ₂
F	Ac-DFFKAFYDKVAEKFKKEAF-NH₂ Ac-DFFKAFY[Cl]DKVAEKFKKEAF-NH ₂

Chromatographic peaks depicted in Fig. 5 were collected, lyophilized, and reconstituted for MALDI-TOF MS analysis. The predominant species present in each fraction is bolded.

of HOCl on the helicity of lipid-free 4F, as measured by CD spectroscopy (Table 3). In contrast to 4F, the helicity of lipid-free native 4F [W→F] was significantly reduced, suggesting a reduction in the α -helical structure of this peptide. 4F [W→F] was also less effective than 4F in clarifying POPC emulsions (Fig. 6B), suggesting a reduction in the amphipathic helical nature of this peptide compared with 4F. Surprisingly, oxidation of 4F [W→F] increased its helicity and capacity to clarify POPC, suggesting an enhanced physical interaction between oxidized peptide and lipid (Table 3, Fig. 6B). Effects of oxidation on the ability of 4F and 4F [W→F] to serve as effectors of cholesterol efflux was tested in cholesterol-loaded THP-1 cells. Cholesterol efflux mediated by native and HOCl-modified 4F was similar (Fig. 7A). Compared with native 4F, cholesterol efflux mediated by native 4F [W→F] was reduced by 56%. There was a tendency for increased cholesterol efflux by 4F [W→F] that was treated with HOCl; however, this was not significantly different from the efflux mediated by native 4F [W→F] (Fig. 7A).

It is possible that native and oxidized peptide concentrations under these conditions might saturate ABCA1-dependent

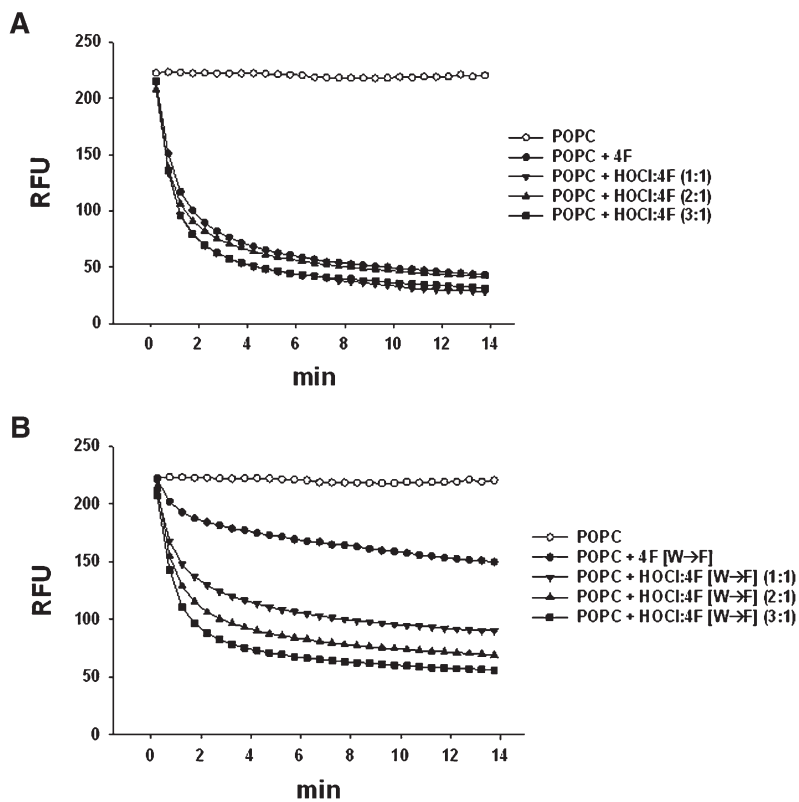


Fig. 6. Effects of HOCl on lipid binding properties of 4F and 4F [W→F]. Effects of HOCl on the ability of 4F and 4F [W→F] to clarify POPC MLVs were tested in vitro. HOCl treatment did not influence 4F-mediated lipid binding and clarification of the phospholipid (panel A). 4F [W→F] was less effective than 4F in clarifying POPC emulsions. Oxidation of 4F [W→F], however, increased its lipid binding interaction with POPC (panel B).

efflux and therefore mask an effect of oxidation on cholesterol efflux. To address this question, we measured the concentration dependence of native and HOCl-modified 4F and 4F [W→F] on cholesterol efflux. 4F induced a concentration-dependent increase in cholesterol efflux that reached a maximum at 50 $\mu\text{g}/\text{ml}$ (Fig. 7B). In this experiment, efflux mediated by HOCl-modified 4F was increased at 25 and 100 $\mu\text{g}/\text{ml}$ compared with native 4F. Consistent with our previous experiment, cholesterol efflux mediated by 4F [W→F] was modest (Fig. 7C). Oxidation of 4F [W→F] did not significantly influence cholesterol efflux, except at the 100 $\mu\text{g}/\text{ml}$ concentration.

DISCUSSION

Neutrophils and macrophages are principal sources of MPO under inflammatory conditions (33, 34). We previously reported that neutrophils interact with endothelial cells and release MPO, resulting in its accumulation in the subendothelial space (35). In this compartment, MPO-derived HOCl reacts with numerous targets,

including amino acids, resulting in altered protein function and cellular injury (5, 36). The MPO-dependent modification of apoA-I structure and function have been studied previously. Several studies show that Cl-Tyr formation in apoA-I is associated with the loss of ABCA1-dependent cholesterol efflux (16, 19, 23). Other data suggest that, although Cl-Tyr formation may serve as a marker for the halogenation of apoA-I, this change does not specifically influence the cholesterol efflux capacity of the apolipoprotein (25). Exposure of recombinant apoA-I mutants that were devoid of Tyr residues to MPO/H₂O₂/Cl⁻ did not prevent the impairment of apoA-I-mediated cholesterol efflux, suggesting a minor role for Tyr modification in the impairment of apoA-I function (25). Rather, data suggest that Trp residues in apoA-I play a critical role in cholesterol efflux. In this regard, it was shown that site-directed mutagenesis of all four Trp residues in apoA-I to leucine resulted in the loss of cholesterol efflux capacity (20). Further, it was shown that MPO oxidized Trp residues in apoA-I, resulting in the formation of mono- and dihydroxytryptophan and a reduction in cholesterol efflux (25). It was proposed that oxidation of Trp alters apoA-I function by inducing a conformational change in the apolipoprotein, resulting in the translocation of modified Trp residues to an aqueous environment (25). More recently, it was suggested that the α -helical content of Trp-free apoA-I mutants is increased compared with native protein (22). This may induce changes in secondary and tertiary structure, resulting in a recombinant protein with properties different from native apoA-I itself (22).

TABLE 3. Percentage helicity of lipid-free 4F and 4F [W→F]

HOCl:Peptide Ratio [mol/mol]	4F	4F [W→F]
0:1	36.7 ± 2.0	14.0 ± 0.2
1:1	30.7 ± 2.9	30.8 ± 1.5 ^a
2:1	37.7 ± 1.8	32.7 ± 0.9 ^a
3:1	41.7 ± 1.6	33.2 ± 2.3 ^a

Data are means ± SEM (n = 3).

^aP < 0.05 denotes a significant difference compared with peptide in the absence of HOCl (0:1 mol/mol).

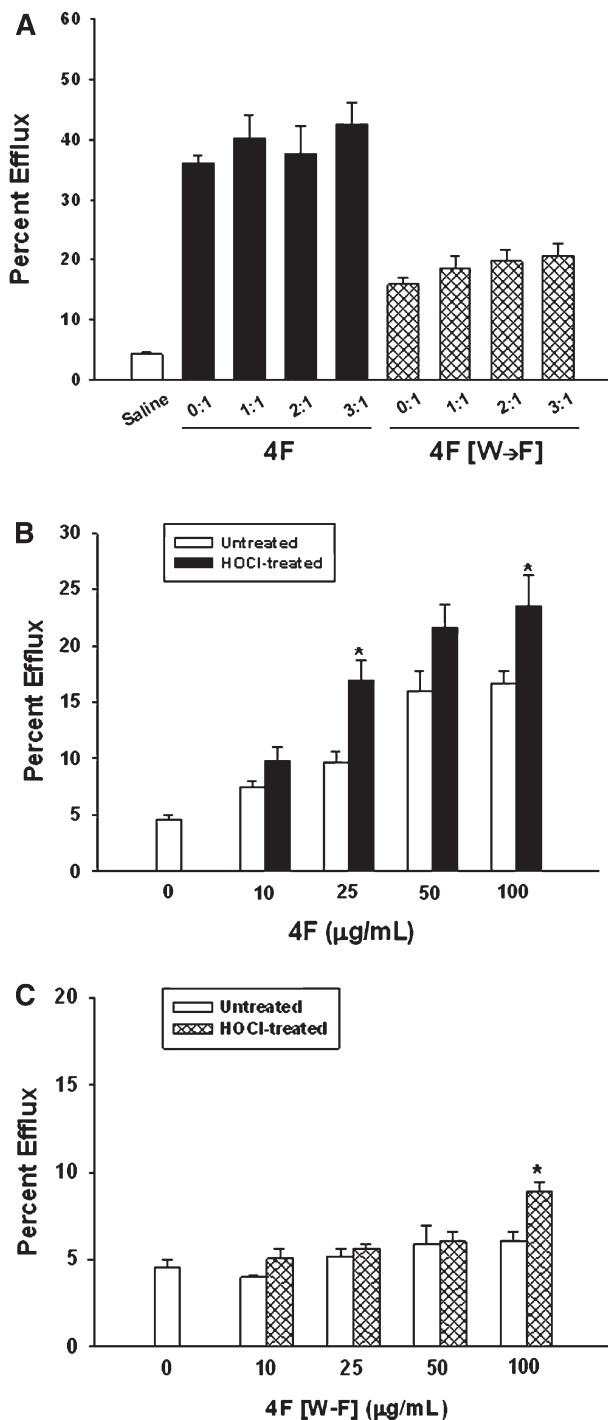


Fig. 7. Effects of HOCl on cholesterol effluxing properties of 4F and 4F [W→F]. The ABCA1-dependent efflux of cholesterol mediated by 4F and 4F [W→F] was monitored in THP-1 monocytes. ³H-cholesterol-loaded cells were incubated with 4F or 4F [W→F] (100 µg/ml each) for 24 h in lipoprotein-depleted medium (panel A). In some experiments, HOCl was incrementally added to 4F or 4F [W→F] resulting in HOCl:peptide molar ratios ranging from 1:1 to 3:1. The ability of these HOCl-modified peptides to mediate cholesterol efflux was monitored. Data are the mean ± SEM (n = 11–12 for each peptide). Efflux data was normalized and expressed as a percentage of total counts effluxed by 4F or 4F [W→F]. Although cholesterol efflux for all treatments was significantly increased compared with saline control, there were no differences in efflux mediated by native and oxidized peptides. Concentration-dependent effects of native and HOCl-modified 4F and 4F [W→F]

Under inflammatory conditions, the trafficking of HDL/apoA-I across the blood vessel wall provides the opportunity for modification by MPO (37). Similarly, 4F administration in vivo is associated with the rapid clearance of the peptide from the circulation and its incorporation in the vascular compartment (38). Because the apoA-I mimetic peptide 4F shares structural similarities with apoA-I, including the presence of redox-sensitive aromatic amino acids, we tested the hypothesis that the peptide serves as a reactive substrate for HOCl. Our data show that 4F competes with APF for reaction with HOCl (Fig. 1). HOCl also altered the physical properties of 4F, resulting in both modification of the native peptide and the formation of new products (Fig. 2). On denaturing SDS-PAGE gels, HOCl reduced the band intensity for native 4F, and this was associated with the formation of a new, higher molecular weight product (Fig. 2). With respect to the latter, mass spectral analyses suggested that HOCl induced the formation of 4F dimers via the cross-linking of the oxidized 4F metabolite Oia. Treatment of 4F with HOCl altered Trp as shown by the decrease of Trp fluorescence (Fig. 4). This modification resulted in the formation of oxidized 4F products in which one or two oxygen atoms were added, but at different positions on the indole ring. This is reflected by the presence of oxidized 4F products with the same molecular weight but with different HPLC retention times (Fig. 3B, Table 1). On the basis of mass spectral analyses, we suggest the formation of various products as shown in Fig. 3D. Overall, the amphipathicity and lipid-associating properties of these modified 4F products were maintained with no change in the makeup of the polar and nonpolar faces, as the Trp residue is present at the polar-nonpolar interface (Fig. 8). Oxidation of the Phe residue on the nonpolar face was observed in two out of seventeen 4F metabolites identified in Table 1. This modification, however, did not alter the helicity of oxidized 4F. Our results are consistent with the idea that the interfacial Trp acts as a substrate for reactive HOCl.

To determine the importance of Trp modification and possible changes in the properties of 4F, the control peptide 4F [W→F] was synthesized by replacing Trp (W) with the aromatic amino acid Phe (F). According to the Wimley and White hydrophobicity scale, next to Trp, Phe is the most hydrophobic amino acid, although unlike Trp, there is no indole NH for this amino acid to orient toward the aqueous environment (39). As shown in Fig. 8A, the only Trp residue in the sequence of 4F is present at the polar-nonpolar interface of the helical wheel representation of 4F. The rate constant for the reaction of HOCl with Trp is approximately 2,500 times faster than that for Tyr and is even greater than that for Phe (21). It follows that Trp is the preferred target for HOCl in 4F. CD studies showed that replacement of Trp with Phe in 4F [W→F] resulted in

on cholesterol efflux are depicted in panels B and C, respectively. Data are the mean ± SEM (n = 6 for each peptide). *P < 0.05 compared with peptide-mediated efflux in the absence of HOCl.

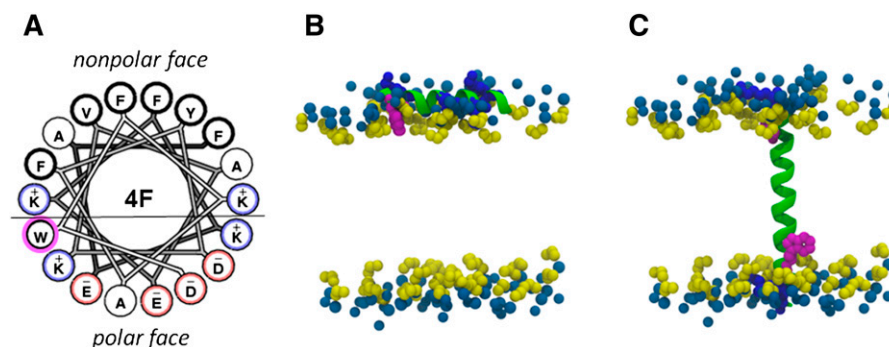


Fig. 8. Molecular dynamics of Trp-containing peptides. The helical wheel diagram of 4F shows the localization of the Trp residue at the polar-nonpolar interface, represented by the black line (panel A). An all atom structure for 4F (panel B) and the Tar chemoreceptor transmembrane TM2 peptide [RFAQWLAVIALVVV-LILLVAWYGIRRM] were obtained by Coarse-Grain Molecular Dynamics simulation (panel C). Hydrophobic residues in 4F and TM2 are represented by the green helices. Lys residues are denoted in deep blue and acidic residues in 4F are not shown in panel B. The position of Trp residues (magenta) in the lipid bilayer are shown in close proximity to the glycerol backbone of POPC (yellow) in both the amphipathic helical 4F and TM2 structures. POPC acyl groups are not shown. Sky blue dots represent PC.

a peptide with reduced helicity compared with 4F. It is proposed that the reduction in α -helical content of 4F [W→F] enhances the exposure of the Tyr residue thus allowing its modification by HOCl. In support of this, we found that HOCl induced the chlorination of Tyr residues in the 4F [W→F] peptide and increased its hydrophobicity. This property was associated with enhanced lipid binding (Fig. 6). Similar to 4F, we also found that 4F [W→F] reduced the HOCl-dependent oxidation of APF in a concentration-dependent manner (Fig. 5A). The ED_{50} s for the inhibition of APF oxidation were similar for both peptides.

Treatment of 4F [W→F] with HOCl did not influence its mobility on SDS gels (Fig. 5B). Chromatographic separation of HOCl-treated 4F [W→F] revealed the formation of new products with a prolonged retention time (Fig. 5D). Mass spectral analyses of HOCl-treated 4F [W→F] revealed that the peptide was more resistant to oxidation than was 4F. Data presented in Table 2 show that HOCl induced the formation of one chlorinated 4F [W→F] metabolite and up to two Phe oxidation products. This, however, changed the spectral properties of this peptide, increased the hydrophobicity of the nonpolar face and thus elution at a higher retention time (Fig. 5C). In contrast, HOCl treatment of 4F resulted in the formation of up to seven oxidation products as well as multiple cleavage products (Table 1).

An additional goal of this study was to test whether the oxidative modification of 4F altered its function, including the ability to mediate ABCA1-dependent cholesterol efflux, analogous to what is reported for apoA-I (15–18, 23, 25). It is interesting to note that in transmembrane domains of membrane spanning α -helices, the amino acid Trp has a unique transmembrane distribution pattern close to the membrane interface (40). It has been suggested that these transmembrane Trp residues impart cytoprotective and antioxidant properties, as the presence of Trp and Tyr in transmembrane proteins protects the surrounding lipid bilayer from peroxidation (41). Fig. 8C

shows the transmembrane TM2 peptide, a component of the Tar chemoreceptor protein, as an example of a single transmembrane domain possessing Trp at the water-lipid interface. Molecular dynamic (MD) simulations of both surface active (4F) and transmembrane (TM2) helices are presented in Fig. 8B, C. The indole moiety of the Trp residue is oriented toward the hydrophobic interior near the interface in both the cases. Modification of Trp by oxidation at the interface is not expected to change the lipid-associating ability either via hydrophobic interaction or via charged residue interactions with the phospholipid head group. In agreement with this, the ability of Trp-modified 4F products to associate with lipids and to act as an acceptor for cholesterol was similar to native 4F. Results of CD studies also showed that HOCl did not significantly alter the helicity of lipid-free 4F. In contrast to 4F, replacement of Trp with Phe in 4F [W→F] reduced its amphipathic properties, as revealed by a diminished capacity to associate with phospholipid and to stimulate ABCA1-mediated cholesterol efflux (Fig. 6). Exposure of 4F [W→F] to HOCl increased both its helicity and lipid-associating ability, but the resulting products were much less effective than native and oxidized 4F as mediators of ABCA1-dependent cholesterol efflux (Fig. 6B, Table 3).

Antiatherogenic and anti-inflammatory mechanisms of 4F have been extensively studied (42). Principal functions ascribed to 4F include the ability to bind lipids, to act as an acceptor for macrophage cholesterol efflux and to reduce atherogenic lesion formation in experimental animals (29, 43). Our data suggest that the sole Trp residue in 4F plays a critical role in these responses, as substitution of Phe for Trp yielded an analog peptide (4F [W→F]) that was less effective in clarifying POPC emulsions and acting as a cholesterol acceptor. Data also suggest 4F possesses antioxidant properties by virtue of its ability to avidly bind oxidized lipids, reduce tissue-associated E06 immunoreactivity and to induce the expression of heme oxygenase-1 and extracellular superoxide dismutase (29, 44, 45). The current study shows that the presence of the Trp residue at

the polar-nonpolar interface of 4F confers an endogenous antioxidant property on 4F. Although the HOCl-induced modification of Trp resulted in the formation of a variety of 4F metabolites, the amphipathicity of these molecules was maintained, thus preserving its lipid-associating property. 4F was equally susceptible to oxidation in the presence of and absence of lipid (Fig. 4A, B). This is consistent with our previous observation that the helicity of 4F is similar in aqueous (45% helicity) and lipid (44% helicity) environments (30). Under both conditions, the interfacial Trp residue is exposed and is susceptible to oxidation. In contrast to studies in apoA-I, we found no evidence for Cl-Tyr formation in 4F (24). Cl-Tyr was observed only in the mutant peptide 4F [W→F] that lacked a Trp residue. The helicity of 4F [W→F] was also reduced compared with 4F, suggesting a lack of amphipathic helical structure capable of associating with lipids and cholesterol effluxing properties. It is likely that Tyr residues in aggregates of 4F [W→F] are readily exposed to HOCl but are effectively shielded in 4F aggregates.

In conclusion, results of the current studies suggest that oxidant scavenging represents an additional antiatherogenic mechanism of apoA-I mimetic peptide action. Oxidation of 4F does not alter its capacity to act as a mediator of cholesterol efflux, thus suggesting a dual functional nature of the peptide. We additionally monitored the HOCl-induced loss of Trp and Tyr absorbance (A_{280}) in 4F and apoA-I. Our results show that the initial rate of decay for both 4F and apoA-I was similar and near maximal after 30 s (Fig. 4B). Under these conditions, the reduction in A_{280} was similar for 4F and apoA-I, suggesting equal susceptibility to HOCl-induced oxidation. In ongoing studies, we are testing whether 4F administration prevents oxidative modifications to apoA-I and loss of HDL function. **■**

The authors thank Dr. Andrea Catta for generating MD simulations of the two membrane active peptides containing Trp.

REFERENCES

- Zhang, R., M. L. Brennan, X. Fu, R. J. Aviles, G. L. Pearce, M. S. Penn, E. J. Topol, D. L. Sprecher, and S. L. Hazen. 2001. Association between myeloperoxidase levels and risk of coronary artery disease. *JAMA*. **286**: 2136–2142.
- Hazen, S. L., and J. W. Heinecke. 1997. 3-Chlorotyrosine, a specific marker of myeloperoxidase-catalyzed oxidation, is markedly elevated in low density lipoprotein isolated from human atherosclerotic intima. *J. Clin. Invest.* **99**: 2075–2081.
- MacCallum, N. S., G. J. Quinlan, and T. W. Evans. 2007. The role of neutrophil-derived myeloperoxidase in organ dysfunction and sepsis. *Intensive Care Med.* **2007**: 173–187.
- Breckwoldt, M. O., J. W. Chen, L. Stangenberg, E. Aikawa, E. Rodriguez, S. Qiu, M. A. Moskowitz, and R. Weissleder. 2008. Tracking the inflammatory response in stroke *in vivo* by sensing the enzyme myeloperoxidase. *Proc. Natl. Acad. Sci. USA*. **105**: 18584–18589.
- Hawkins, C. L., D. I. Pattison, and M. J. Davies. 2003. Hypochlorite-induced oxidation of amino acids, peptides and proteins. *Amino Acids*. **25**: 259–274.
- Yang, C. Y., Z. W. Gu, M. Yang, S. N. Lin, A. J. Garcia-Prats, L. K. Rogers, S. E. Welty, and C. V. Smith. 1999. Selective modification of apoB-100 in the oxidation of low density lipoproteins by myeloperoxidase *in vitro*. *J. Lipid Res.* **40**: 686–698.
- Carr, A. C., T. Tjjerina, and B. Frei. 2000. Vitamin C protects against and reverses specific hypochlorous acid- and chloramine-dependent modifications of low-density lipoprotein. *Biochem. J.* **346**: 491–499.
- Chantepie, S., E. Malle, W. Sattler, M. J. Chapman, and A. Kontush. 2009. Distinct HDL subclasses present similar intrinsic susceptibility to oxidation by HOCl. *Arch. Biochem. Biophys.* **487**: 28–35.
- Panzenboeck, U., S. Raitmayer, H. Reicher, H. Lindner, O. Glatter, E. Malle, and W. Sattler. 1997. Effects of reagent and enzymatically generated hypochlorite on physicochemical and metabolic properties of high density lipoproteins. *J. Biol. Chem.* **272**: 29711–29720.
- Malle, E., G. Marsche, U. Panzenboeck, and W. Sattler. 2006. Myeloperoxidase-mediated oxidation of high-density lipoproteins: fingerprints of newly recognized potential proatherogenic lipoproteins. *Arch. Biochem. Biophys.* **445**: 245–255.
- Undurti, A., Y. Huang, J. A. Lupica, J. D. Smith, J. A. DiDonato, and S. L. Hazen. 2009. Modification of high density lipoprotein by myeloperoxidase generates a pro-inflammatory particle. *J. Biol. Chem.* **284**: 30825–30835.
- Marsche, G., A. Hammer, O. Oskolkova, K. F. Kozarsky, W. Sattler, and E. Malle. 2002. Hypochlorite-modified high density lipoprotein, a high affinity ligand to scavenger receptor class B, type I, impairs high density lipoprotein-dependent selective lipid uptake and reverse cholesterol transport. *J. Biol. Chem.* **277**: 32172–32179.
- Guertin, F., S. Brunet, D. Lairon, and E. Levy. 1997. Oxidative tyrosylation of high density lipoprotein impairs biliary sterol secretion in rats. *Atherosclerosis*. **131**: 35–41.
- Pirillo, A., P. Uboldi, and A. L. Catapano. 2010. Dual effect of HOCl in the modification of high density lipoproteins. *Biochem. Biophys. Res. Commun.* **403**: 447–451.
- Shao, B., S. Pennathur, I. Pagani, M. Oda, J. L. Witztum, J. F. Oram, and J. W. Heinecke. 2010. Modifying apolipoprotein A-I by malondialdehyde, but not by an array of other reactive carbonyls, blocks cholesterol efflux by the ABCA1 pathway. *J. Biol. Chem.* **285**: 18473–18484.
- Shao, B., C. Bergt, X. Fu, P. Green, J. C. Voss, M. N. Oda, J. F. Oram, and J. W. Heinecke. 2005. Tyrosine 192 in apolipoprotein A-I is the major site of nitration and chlorination by myeloperoxidase, but only chlorination markedly impairs ABCA1-dependent cholesterol transport. *J. Biol. Chem.* **280**: 5983–5993.
- Zheng, L., B. Nukana, M. L. Brennan, M. Sun, M. Goormastic, M. Settle, D. Schmitt, X. Fu, L. Thomson, P. L. Fox, et al. 2004. Apolipoprotein A-I is a selective target for myeloperoxidase-catalyzed oxidation and functional impairment in subjects with cardiovascular disease. *J. Clin. Invest.* **114**: 529–541.
- Shao, B., G. Caviglioglio, N. Brot, M. Oda, and J. W. Heinecke. 2008. Methionine oxidation impairs reverse cholesterol transport by apolipoprotein A-I. *Proc. Natl. Acad. Sci. USA*. **105**: 12224–12229.
- Bergt, C., S. Pennathur, X. Fu, J. Byun, K. O. O'Brien, T. O. McDonald, P. Singh, G. M. Anantharamaiah, A. Chait, J. Brunzell, et al. 2004. The myeloperoxidase product hypochlorous acid oxidizes HDL in the human artery wall and impairs ABCA1-dependent cholesterol transport. *Proc. Natl. Acad. Sci. USA*. **101**: 13032–13037.
- Peng, D. Q., G. Brubaker, Z. Wu, L. Zheng, B. Willard, M. Kinter, S. L. Hazen, and J. D. Smith. 2008. Apolipoprotein A-I tryptophan substitution leads to resistance to myeloperoxidase-mediated loss of function. *Arterioscler. Thromb. Vasc. Biol.* **28**: 2063–2070.
- Pattison, D. I., and M. J. Davies. 2001. Absolute rate constants for the reaction of hypochlorous acid with protein side-chains and peptide bonds. *Chem. Res. Toxicol.* **14**: 1453–1464.
- Shao, B., C. Tang, J. W. Heinecke, and J. F. Oram. 2010. Oxidation of apolipoprotein A-I by myeloperoxidase impairs the initial interactions with ABCA1 required for signaling and cholesterol export. *J. Lipid Res.* **51**: 1849–1858.
- Zheng, L., M. Settle, G. Brubaker, D. Schmitt, S. L. Hazen, J. D. Smith, and M. Kinter. 2005. Localization of nitration and chlorination sites on apolipoprotein A-I catalyzed by myeloperoxidase in human atheroma and associated oxidative impairment in ABCA1-dependent cholesterol efflux from macrophages. *J. Biol. Chem.* **280**: 38–47.
- Bergt, C., X. Fu, N. P. Huq, J. Kao, and J. W. Heinecke. 2004. Lysine residues direct the chlorination of tyrosines in YXXK motifs of apolipoprotein A-I when hypochlorous acid oxidizes high density lipoprotein. *J. Biol. Chem.* **279**: 7856–7866.

25. Peng, D. Q., Z. Wu, G. Brubaker, L. Zheng, M. Settle, E. Gross, M. Kinter, S. L. Hazen, and J. D. Smith. 2005. Tyrosine modification is not required for myeloperoxidase-induced loss of apolipoprotein A-I functional activities. *J. Biol. Chem.* **280**: 33775–33784.
26. Navab, M., G. M. Anantharamaiah, S. T. Reddy, B. J. Van Lenten, G. Hough, A. Wagner, K. Nakamura, D. W. Garber, G. Datta, J. P. Segrest, et al. 2004. Human apolipoprotein AI and A-I mimetic peptides: potential for atherosclerosis reversal. *Curr. Opin. Lipidol.* **15**: 645–649.
27. Smythies, L. E., C. R. White, A. Maheshwari, M. Palgunachari, G. M. Anantharamaiah, M. Chaddha, A. R. Kurundkar, and G. Datta. 2010. The apolipoprotein A-I mimetic, 4F, alters the function of human monocyte-derived macrophages. *Am. J. Physiol. Cell Physiol.* **298**: C1538–C1548.
28. Wool, G. D., C. A. Reardon, and G. S. Getz. 2008. Apolipoprotein A-I mimetic peptide helix number and helix linker influence potentially anti-atherogenic properties. *J. Lipid Res.* **49**: 1268–1283.
29. Van Lenten, B. J., A. C. Wagner, C. L. Jung, P. Ruchala, A. J. Waring, R. I. Lehrer, A. D. Watson, S. Hama, M. Navab, G. M. Anantharamaiah, et al. 2008. Anti-inflammatory apoA-I-mimetic peptides bind oxidized lipids with much higher affinity than human apoA-I. *J. Lipid Res.* **49**: 2302–2311.
30. Datta, G., M. Chaddha, S. Hama, M. Navab, A. M. Fogelman, D. W. Garber, V. K. Mishra, R. M. Epand, R. F. Epand, S. Lund-Katz, et al. 2001. Effects of increasing hydrophobicity on the physical-chemical and biological properties of a class A amphipathic helical peptide. *J. Lipid Res.* **42**: 1096–1104.
31. Meriwether, D., S. Imaizumi, V. Grijalva, G. Hough, L. Vakili, G. M. Anantharamaiah, R. Farias-Eisner, M. Navab, A. M. Fogelman, S. T. Reddy, et al. 2011. Enhancement by LDL of transfer of L-4F and oxidized lipids to HDL in C57BL/6J mice and human plasma. *J. Lipid Res.* **52**: 1795–1809.
32. Kritharides, L., A. Christian, G. Stoudt, D. Morel, and G. H. Rothblat. 1998. Cholesterol metabolism and efflux in human THP-1 macrophages. *Arterioscler. Thromb. Vasc. Biol.* **18**: 1589–1599.
33. Rodrigues, M. R., D. Rodriguez, M. Russo, and A. Campa. 2002. Macrophage activation includes high intracellular myeloperoxidase activity. *Biochem. Biophys. Res. Commun.* **292**: 869–873.
34. Odobasic, D., A. R. Kitching, T. J. Semple, and S. R. Holdsworth. 2007. Endogenous myeloperoxidase promotes neutrophil-mediated renal injury, but attenuates T-cell immunity inducing crescentic glomerulonephritis. *J. Am. Soc. Nephrol.* **18**: 760–770.
35. Baldus, S., J. P. Eiserich, A. Mani, L. Castro, M. Figueroa, P. Chumley, W. Ma, A. Tousson, C. R. White, D. C. Bullard, et al. 2001. Endothelial transcytosis of myeloperoxidase confers specificity to vascular ECM proteins as targets of tyrosine nitration. *J. Clin. Invest.* **108**: 1759–1770.
36. Szuchman-Sapir, A. J., D. I. Pattison, N. A. Ellis, C. L. Hawkins, M. J. Davies, and P. K. Witting. 2008. Hypochlorous acid oxidizes methionine and tryptophan residues in myoglobin. *Free Radic. Biol. Med.* **45**: 789–798.
37. Barter, P. J., S. Nicholls, K. A. Rye, G. M. Anantharamaiah, M. Navab, and A. M. Fogelman. 2004. Antiinflammatory properties of HDL. *Circ. Res.* **95**: 764–772.
38. Dai, L., G. Datta, Z. Zhang, R. Patel, J. Honavar, S. Modi, M. Chaddha, M. Palgunachari, J. M. Wyss, H. Gupta, et al. 2010. The apolipoprotein A-I mimetic peptide 4F prevents defects in vascular function in endotoxemic rats. *J. Lipid Res.* **51**: 2695–2705.
39. Wimley, W. C., and S. H. White. 1996. Experimentally determined hydrophobicity scale for proteins at membrane interfaces. *Nat. Struct. Biol.* **3**: 842–848.
40. Hall, B. A., J. A. Armetage, and M. S. P. Sansom. 2011. Transmembrane helix dynamics of bacterial chemoreceptors support a piston model of signalling. *PLoS Comput. Biol.* **7**: e1002204.
41. Moosmann, B., and C. Behel. 2000. Cytoprotective and anti-oxidant functions of Trp and Tyr residues in transmembrane proteins. *Eur. J. Biochem.* **267**: 5687–5692.
42. White, C. R., G. Datta, A. Wake, Z. Zhang, H. Gupta, D. W. Garber, V. K. Mishra, M. N. Palgunachari, S. P. Handattu, M. Chaddha, et al. 2008. HDL therapy for cardiovascular diseases: the road to HDL mimetics. *Curr. Atheroscler. Rep.* **10**: 405–412.
43. Navab, M., G. M. Anantharamaiah, S. Hama, D. W. Garber, M. Chaddha, G. Hough, R. Lallone, and A. M. Fogelman. 2002. Oral administration of an Apo A-I mimetic peptide synthesized from D-amino acids dramatically reduces atherosclerosis in mice independent of plasma cholesterol. *Circulation.* **105**: 290–292.
44. Buga, G. M., J. S. Frank, G. A. Mottino, A. Hakhamian, A. Narasimha, A. D. Watson, B. Yekta, M. Navab, S. T. Reddy, G. M. Anantharamaiah, et al. 2008. D-4F reduces EO6 immunoreactivity, SREBP-1c mRNA levels, and renal inflammation in LDL receptor-null mice fed a Western diet. *J. Lipid Res.* **49**: 192–205.
45. Kruger, A. L., S. Peterson, S. Turkseven, P. M. Kaminski, F. F. Zhang, S. Quan, M. S. Wolin, and N. G. Abraham. 2005. D-4F induces heme oxygenase-1 and extracellular superoxide dismutase, decreases endothelial cell sloughing, and improves vascular reactivity in rat model of diabetes. *Circulation.* **111**: 3126–3134.